Robotics and Computer–Integrated Manufacturing 91 (2025) 102843

Contents lists available at ScienceDirect

Robotics and Computer-Integrated Manufacturing

journal homepage: www.elsevier.com/locate/rcim

Enhancing compliant gripper performance: Exploiting electro-adhesion to increase lifting force over grasping force

Amedeo Carloni [a,*], Marcello Valori [b], Federico Bertolucci [a], Lorenzo Agostini [a], Giovanni Berselli [c], Irene Fassi [d], Lorenzo Molinari Tosatti [d], Rocco Vertechy [a,d]

[a] Dept. of Mechanical Engineering, University of Bologna, Bologna, 40126, Italy
[b] ENEA, Technology Transfer Directorate, Italian National Agency for New Technologies, Energy and Sustainable Economic Development, Via Martiri di Monte Sole 4, Bologna, 40129, Italy
[c] Dept. of Mechanical, Energy, Management and Transportation Engineering, University of Genova, Genova, 16145, Italy
[d] CNR, Institute of Intelligent Industrial Technologies and Systems for Advance Manufacturing, Via A. Corti 12, Milano, 20133, Italy

ARTICLE INFO

Keywords:
Compliant gripper
Elastomer characterization
Electro-adhesion
Fin ray effect
Soft gripper
Urethane rubber
Hyperelastic material

ABSTRACT

On the landscape of solutions to deal with delicate objects, the development and use of soft grippers is a topic of increasing interest, with a large number of prototypes proposed by the research community employing non-linear soft materials and based on diverse actuation means. However, increasing compliance usually leads to the reduction of lifting capacity. As a recent promising approach, shear forces exerted by a soft gripper can be enhanced by exploiting the electro-adhesion (EA) effect. Following this research trend, this paper proposes a new gripper that combines a compliant finger structure, with geometry taken from the FESTO FinRay but made of a softer material (a urethane rubber), and custom EA pads that are placed on the fingers at the interface with the grasped object. Following hyper-elastic model identification of the considered material and preliminary functional verification of gripper design via finite element simulations, the gripper is then manufactured and tested by means of a specific setup, replicating the grasping and lifting of cylindrical objects with different diameters. The results clearly show that the new gripper makes it possible to generate holding forces similar to those of the FESTO FinRay, but with significantly lower pressures on the grasped object (77 % less). Besides enabling the handling of more fragile items, the drastic increase in gripper compliance also results in lower mechanical actuation force (namely, 71 % less of gripping energy) required to generate the same holding force, with a consequent reduction of operation costs and sustainability of its application.

1. Introduction

Grasping and manipulation still stand among the most relevant research topics in robotics. In particular, it is widely recognized that conventional rigid grippers are characterized by low flexibility, resulting in a major limitation in the manipulation of large varieties of different objects [1-3]. Underactuated adaptive grippers partially overcome this limit, featuring the capability of wrapping around objects of unknown geometry, without dedicated controllers [4] and sensors [5-7]. Within this category, a widespread approach relies on the use of soft materials for the gripper structure, which minimizes the need for expensive control systems and sensors [8-12]. Soft grippers (SGs) can, indeed, adapt to irregular surfaces, enabling the grasping and handling of objects with different shapes, sizes, and materials [13-15]. SGs are typically constituted by compliant materials, such as elastomers, that distribute forces uniformly, which can also be advantageous in those environments characterized by high safety standards like human-robot physical interaction. In the research landscape, many SGs have demonstrated their versatility in grasping different shapes based on a variety of actuation methods, such as pneumatic, cable-drive, shape memory alloy/polymer, and dielectric elastomer transducer (DET) technologies [16-19]. However, those SGs typically feature the drawback of exhibiting relatively low lifting forces. Electro-adhesion (EA) is an electrically controllable astrictive prehension [20] method that exploits electrostatic forces to grab objects of various shapes and materials. One of the main advantages of implementing EA in gripping devices stands in the possibility of generating high shear forces with negligible compression [21] on the grasped item. For this reason, EA is one of the most

* Corresponding author.
E-mail address: amedeo.carloni2@unibo.it (A. Carloni).

https://doi.org/10.1016/j.rcim.2024.102843
Received 26 July 2024; Accepted 26 July 2024
Available online 10 August 2024

promising technologies to increase the lifting capability of compliant grippers significantly. As compared to other approaches, including EA in SGs requires relatively low design efforts, as EA pads are electrically activated, non-invasive and characterized by high application flexibility. Due to these reasons, several EA-based grippers were recently proposed and implemented [22-25]. Although demonstrating high lifting capacity and versatility, the application of these designs is however only limited to pick-and-place applications, with little possibility of object manipulation. The same limitation persists in [26], even though a promising and versatile combined DET-EA soft gripper with intrinsic actuation is proposed. In [27], a soft pneumatically actuated gripper with EA pads is presented, which however requires two different power sources. An electrostatic SG combined with the gecko effect is proposed in [28], aimed at increasing the performance of the adhesive effect on rough surfaces; however, this solution uses a tendon-driven actuation, which requires a non-trivial control. A shape-adaptive SG, inspired by the FinRay Effect® [29,30] and augmented with EA functionality, called "FinEA", is proposed in [31]. Based on a modified geometry of the original FinRay design by FESTO, this gripper comprises a finger structure made by a compliant elastomeric V-shape shell with hinged rigid plastic ribs, and a silicone-based stretchable EA pad realized via blade coating and screen printing. Although providing the capability of grasping convex and large objects, the major portion (> 60 %) of the shear-lifting force of this SG is however provided by the intrinsic significant tackiness and friction of the silicone pad (rather than from the EA effect), which typically lead to the difficult and slow release of the grasp upon command. Moreover, the relation between the holding force (FH, which is a measure of the lifting capability) and the grasping force (FG, which is the clamping force provided by the mechanical actuation that controls finger motion) of this SG is not provided, which does not make it possible to effectively assess the capabilities of handling fragile and soft objects. In this work, a new FinEA design is proposed which comprises: 1) a monolithic deformable finger structure, with the original geometry and size of the FESTO FinRay but made of a softer elastomeric material in terms of shore hardness scale (namely, a urethane rubber), which is easier to realize and not prone to hinge disassembly; 2) a flexible but inextensible EA pad with polyimide (PI) grasping interface, which provides higher (> 300 %) electrically-induced shear-lifting forces and quicker release of the grasp upon command. In particular, the development of this new gripper aimed at increasing the FH to FG ratio of the original FESTO Fin Ray, so as to enhance the handling of fragile and soft objects as well as to reduce the requirements of the actuator controlling finger motion. The paper is organized as follows: after introducing the concept design, the experimental characterization and hyper-elastic model identification of the elastomeric material chosen for the realization of the compliant finger structure are addressed, which are then used for a preliminary assessment of the new FinEA via Finite Element Analyses (FEA); afterward, the fabrication of the gripper is described, including both the FinRay structure and the EA pad, as well as their integration; last, the experimental campaign conducted to characterize the new FinEA as well as the original version by FESTO is presented, followed by the discussion of results and the conclusions.

2. Gripper design

The proposed FinEA gripper is shown in Fig. 1. It comprises two identical FinRay fingers, with the same geometry and dimensions as the original FESTO FinRay (adaptive gripper finger DHAS-GF-80-U-BU) but made with a softer material (the urethane rubber PMC™−780 Dry by Smooth-On), each integrating a flexible but inextensible EA pad. The structure of finger rigid supports features two protrusions (additively manufactured in Rigid 4000® with a Formlabs 2 printer) to mate with the inner space between the first two ribs of the finger. The two fingers are suitable for integration on commercial robot grippers with sliding jaws. In particular, we considered the FinEA fingers installed on the FRANKA EMIKA robot arm hand (Fig. 1(a)). Regarding the identical EA pads (Fig. 1(b)), they feature a multilayer architecture with interdigitated electrode geometry as shown in Fig. 1(c).

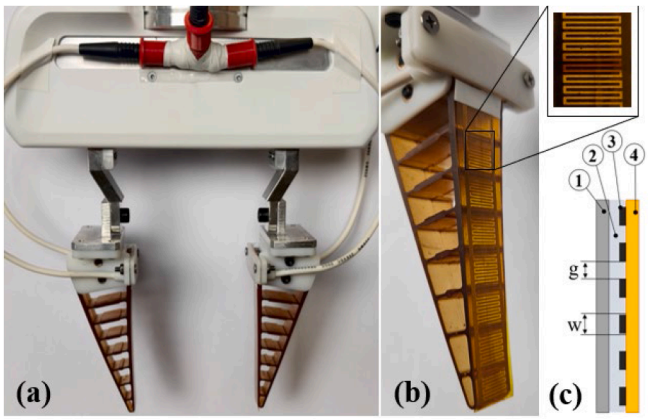

Fig. 1. (a) Proposed FinEA fingers integrated on a FRANKA EMIKA robot arm gripper. (b) Details of a gripper finger, magnification on the interdigitated geometry. (c) Interdigitated geometry cross-section: 1) double-coated polyester silicone tape (94 μm); 2) insulating PDMS layer (100 μm); 3) electrode; 4) PI film (25 μm).

The main dielectric layer (namely, the one contacting the objects to be grasped) is made of a commercial PI film with 25 μm thickness (Caplinq PIT1N/210); the interdigitated electrodes are made of inkjet-printed silver (Anapro DGP 40LT-15C) with width, $w = 400$ μm, and gap, $g = 400$ μm; the backing encapsulation layer having a thickness of 100 μm is made of blade-coated Polydimethylsiloxane (PDMS; Wacker Silpuran 6000/05); the bonding layer consists of a commercial double-coated polyester silicone tape (Nitto P-905) with a thickness of 94 μm. Each EA pad has an active area of L x W = 10×70 mm^2 and is provided with inkjet-printed conductive paths linking it, by press contact, to the electrical connections that are directly embedded on the finger rigid supports.

3. Finger material selection and characterization

Material choice plays a fundamental role in the design of EA-based SGs. The FinRay fingers hosting the EA pads must, on the one hand, be soft to conform to the object with maximal contact area (thereby enhancing EA forces) and minimal normal pressure (thus, ensuring a delicate touch), while, on the other hand, feature a certain level of stiffness to avoid finger bending due to external manipulation forces (like those related to object weight and due to gravity or acceleration). In view of these considerations, the urethane rubber PMC™−780 Dry by Smooth-On was selected as the finger material for its strength and stiffness in the desired range (6.2 MPa tensile strength, 750 % elongation at break, 80A shore hardness, and 2.8 MPa 100 % modulus). Although PMC™−780 Dry has already been used for the implementation of SGs [32], detailed mechanical characterization for soft system design and simulation (as it is available for silicones with hardness in the range from 2 to 44 Shore A [33]) is however still lacking. In this context, the following subsections report the results of the experimental testing and constitutive model identification activities that have been conducted to characterize PMC™−780 Dry, as well as the simulation activities performed to validate the new FinEA gripper behaviour.

3.1. Fabrication of the specimen

Mechanical characterization of the considered PMC™−780 Dry was conducted on five identical specimens with geometry and dimensions chosen as per method A of the ASTM D412 standard; in particular, according to the "Die C" shape with a thickness of 3 mm, a total length of 115 mm and a length of the narrow section of 33 mm, as shown in Fig. 2

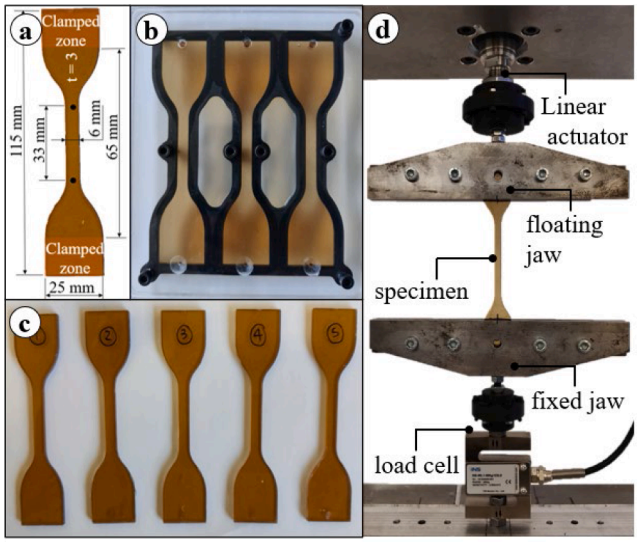

Fig. 2. (a) Dumbbell specimen's geometry and dimensions. (b) Sample Moulds. (c) Five tested specimens. (d) Uniaxial tensile test setup.

(a). A Markforged-Mark Two™ 3D printer was used to fabricate the negative molds in which the two-part (A and B) urethane liquid rubber was poured (see Fig. 2(b)). As recommended by the manufacturer, the mixture was prepared in a 2A:1B ratio by weight. To increase homogeneity and prevent bubble formation, the mixture was subjected to mixing and de-gassing, respectively for three and four minutes, with a THINKY ARE-250 mixer. Then, it was carefully poured into the molds with a syringe and cured at room temperature for 48 h before demolding.

3.2. Uniaxial tensile test

The tensile tests were carried out at 22 °C ambient temperature, on a custom stage (Fig. 2(d)) actuated by a Parker ETH050M05 linear actuator (3 kN maximum force, ± 0.03 mm accuracy) equipped with two jaws: one moved by the actuator output, while the other fixed to the stage frame through a NS-WL1 load cell (50 kg capacity, ± 0.001 N accuracy). Tests were conducted at constant speed from a stretch equal to one up to a maximum value of 1.43. To assess strain-rate dependency, three different speeds were considered (120, 240 and 360 mm/min). For appropriate testing:

- Each specimen was placed inside the jaws by following a marker reference drawn on it to ensure the right amount of clamped area as well as straightness.
- The tightening of the screw's jaw was made by using a torque wrench to 2.5 Nm.
- Each specimen was preloaded with 0.5 N to ensure it was not slack before starting the extension.

To assess reliability, five trials were carried out for each of the five identical specimens tested at the three different speeds. The resulting stress-stretch loading curves are reported in Fig. 3, with one plot for each different speed, blue line for the mean values and shaded green area for the standard deviation.

As shown, the manufactured specimens feature a rather repeatable non-linear elastic response that is negligibly affected by strain rate (at the highest level of stretch, the standard deviation was: 0.13, 0.12 and 0.14 Mpa, respectively for the deformation speeds 120, 240 and 360 mm/min).

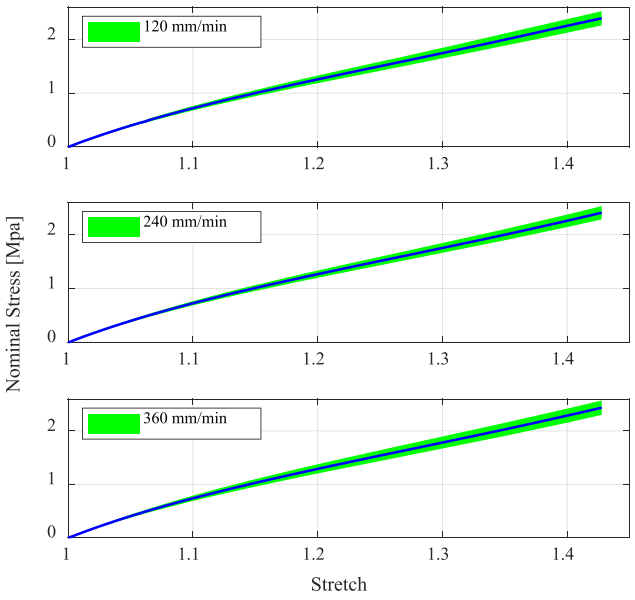

Fig. 3. PMC™−780 Dry stress-stretch loading curves for tensile tests at different strain rates: mean value in blue solid line; standard deviation in a green shaded area.

3.3. Hyperelastic constitutive model identification

The non-linear elastic response of rubber is typically well represented by incompressible hyperelastic models with a strain energy density function, W, formulated in terms of deformation invariants and material constitutive parameters [34]. These models make it possible to find analytical expressions of the stress-stretch response under the simple loading conditions considered for the characterization tests, which can then be easily fitted to experimental data to identify material constitutive parameters [35]. For uniaxial tensile tests, the nominal longitudinal stress (σ) vs. longitudinal stretch (λ) relation follows as [36]:

$$\sigma = 2\left(\lambda - \frac{1}{\lambda^{-2}}\right) \cdot \left(\frac{\partial W}{\partial I_1} + \frac{1}{\lambda}\frac{\partial W}{\partial I_2}\right) \tag{1}$$

with I_1 and I_2 being the Cauchy-Green invariants, expressed by the relations:

$$I_1 = \lambda^2 + \frac{1}{\lambda}, \quad I_2 = 2\lambda^2 + \frac{1}{\lambda^2} \tag{2}$$

and with W being chosen among one of the following forms (out of many others):

- 3rd order Mooney-Rivlin:

$$W = C_{10}(I_1 - 3) + C_{01}(I_2 - 3) + C_{20}(I_1 - 3)^2 \tag{3}$$

- 3rd order Yeoh:

$$W = C_{10}(I_1 - 3) + C_{20}(I_1 - 3)^2 + C_{30}(I_1 - 3)^3 \tag{4}$$

- Ogden:

$$W = \sum_{p=1}^{n} \frac{\mu_p}{\alpha_p}\left[\lambda_1^{\alpha_p} + \lambda_2^{\alpha_p} + \lambda_3^{\alpha_p} - 3\right] \tag{5}$$

- Pucci Saccomandi:

$$W = -\frac{\mu}{2}J_m \ln\left(1 - \frac{I_1 - 3}{J_m}\right) + C_2 \ln\left(\frac{I_2}{3}\right) \quad (6)$$

Fitting the model to the mean experimental curve acquired at 120 mm/min (which is the one that closely resembles the operating condition of the gripper studied in this work) provides the results of Fig. 4 along with the constitutive parameters reported in Table 1, for each of the considered strain energy functions.

Computation has been performed with the MATLAB® *lsqcurvefit* function, which additionally gives the *MSD* error (also reported in Table 1) highlighting the best fit of the 3rd order Yeoh constitutive relation. For verification, the same experimental stress-stretch curve was imported in the MCalibration® software by PolymerFEM® and used to identify the considered constitutive model parameters, which provided similar results. Additionally, the tensile test was simulated through a finite element (FE) model using the 3rd-order Mooney-Rivlin strain energy density with the parameters reported in Table 1. Results are also shown in Fig. 4, which highlights good agreement with both experiments and the analytical model.

4. Finger finite element analyses

To verify the effect of the selected material on the desired gripper softening, a FE simulation of the Fin Ray geometry made of PMC™−780 Dry was performed before fabrication and compared with the experimental data acquired on the original finger made by FESTO (tested with the setup described in Section 6.1). In particular, the grasps of four different cylindrical objects with diameters 50, 60, 70 and 80 mm were investigated. For the sake of simplicity, a symmetric grasp was considered and studied with a single finger on a half of the object fixed to the ground frame. With the Fin Ray base undergoing a 20 mm displacement (in the direction orthogonal to the undeformed contact surface of the finger) to grasp the object, the grasping force (FG, in the direction of motion) was selected as the parameter for assessment. The results reported in Fig. 5 clearly highlight that the modified Fin Ray finger provides a FG that is about 77% lower than that of the original commercialized by FESTO. This results in higher compliance, confirming PMC™−780 Dry as a good material choice. As can be expected: for both original and modified Fin Ray fingers, the greater the diameter of the cylindrical object, the larger the deformation of the gripper and, thus, the reaction force.

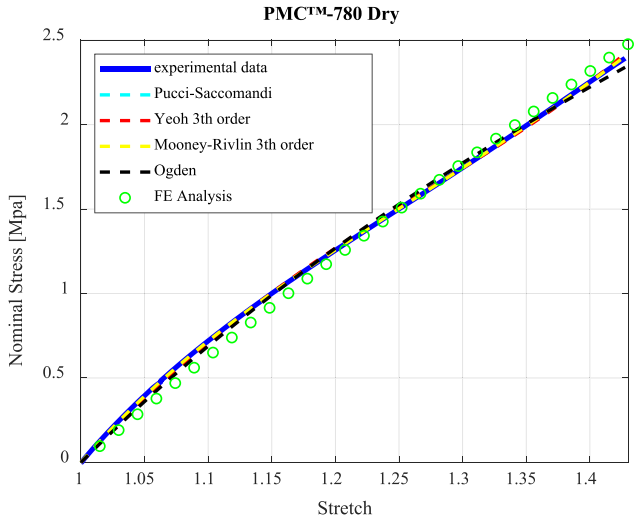

Fig. 4. Comparison between experimental data and predictions from analytical as well as FE models.

Table 1
Constitutive model constants obtained from PMC™−780 Dry tensile testing.

Model	*Parameters [Mpa]*	*MSD*
Pucci-Saccomandi	$\mu = 0.933$ $J_m = 1.272$ $C_2 = 2.575$	0.08
Yeoh 3rd order	$C_{10} = 1.322$ $C_{20} = -0.354$ $C_{30} = 0.518$	0.008
Mooney-Rivlin 3rd order	$C_{10} = 1.220$ $C_{01} = 0.05$ $C_{20} = 0.01$	0.07
Ogden	$\mu_1 = 1.063$ $\alpha_1 = 1.196$ $\mu_2 = 1.196$ $\alpha_2 = 2.593$ $\mu_3 = 0.915$ $\alpha_3 = 0.816$	0.09

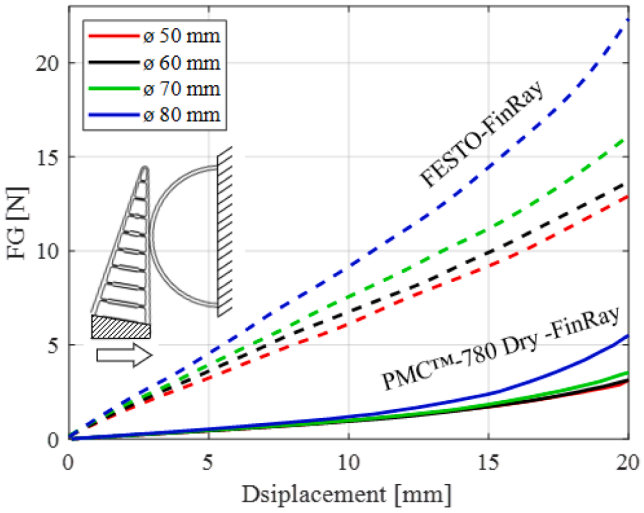

Fig. 5. Fin Ray fingers' comparison: experiments of the original by FESTO vs. simulations of the modified version made of the softer material PMC™−780 Dry.

For completeness, FE analyses on Ansys® have been conducted according to the following settings:

1) *Mechanical static structural model:* the Fin Ray finger and cylindrical object geometry were imported into Design Modeler, and a nonlinear elastic behaviour with a three-parameter Mooney-Rivlin strain energy function with coefficients reported in Table 1 was assigned to the finger, while a rigid behaviour was assigned to the cylindrical object.
2) *Meshing:* nonlinear mechanical physics, quadratic elements Hex-Dominant type with a size of 0.8 mm and aggressive mechanical error limits was set.
3) *Analysis settings:* Auto time stepping on, initial time step and minimum time step in the range 0.001–0.01, maximum time step in the range 0.01–0.05; large deflection on; APDL command Keyopt 6 was inserted to avoid unrealistic behaviour and instability at large deflections.
4) *Boundary conditions and loads:* Static structural; 20 mm horizontal displacement on the gripper's faces that are in contact with the basement in the real set up; fixed support applied to the internal surface of the cylindrical object.
5) *Modelling contact:* the contact between the Fin Ray and the target object was defined as frictional with asymmetric option to minimize penetration, which results in more accurate results and realistic behaviour; contacting meshes were defined with a pinball radius (sphere of influence) of 2 mm; static and dynamic friction coefficients were experimentally determined and respectively set to 0.51 and 0.26; a Pure Penalty method with a Normal Stiffness set to 0.05 (typical of soft material) was chosen to help convergence.

5. Gripper fabrication

Finger prototyping started with the design of the mold, made of two subparts, a lower one (A) and an upper one (B) (Fig. 6). Aiming at high-level surface finishing, both the parts were fabricated by means of a stereolithography (SLA) printing machine (Form 2 by Formlabs). The resin used is the High Temp®, providing high layer resolution (25 μm), as well as good thermal stability and stiffness. Precise mate of the two subparts relies on three centering dowel pins made of hardened steel; a set of four inserts fixed to subpart A was used in combination with the screws as an extractor for subpart B. Tight mold closure is ensured by six screws uniformly distributed. Optimal positioning of the casting and air outlet channels is fundamental for homogeneous mold filling. Accordingly, a single casting channel, with a connection for the injection syringe on the top surface of subpart B, ensures bottom-up mold filling; whereas, to avoid the inclusion of air bubbles, an outlet channel is located on each of the ribs of the Fin Ray, in sub part B of the mold. Two sprues are added on the base and on the tip of the mold to prevent shrinkage. The casted material (PMC™−780 Dry) is the same of the dumbbell specimens described in Section 3.1, as well as the casting preparation and procedure, with the exception of the additional application of the Universal™ Mold Release agent by Smooth-On on the mold before casting.

The EA pads were manufactured via the rapid fabrication procedure described in [24]. After realization, they were finely cut with a laser plotter (Epilog Fusion M32) and bonded to the whole gripping area of the Fin Ray finger via a double-coated polyester silicone tape (P-905 by Nitto). This ensures an effective electro-adhesive action for every level of finger deflection.

6. Test and results

6.1. Experimental setup

To quantitatively evaluate the performance of the new FinEA finger, both grasping (i.e., clamping) and holding (i.e., breakaway) forces generated on cylindrical objects with different diameters were measured on the custom set-up, shown in Fig. 7, comprising:

two orthogonally-placed identical linear motion stages, featuring ACME screw transmissions driven by rotary stepper motors, with the first one used to move the finger along the X direction (namely, the grasping direction) and the second one used to move the cylindrical object in the Y direction (namely, the holding direction); an “S” type load cell (NS-WL1–10kg123L0) used to measure the grasping force (FG) generated by the FinEA finger along the X direction; a shear beam load cell (20 kg-3134-CZL635) to measure the holding force (HF) resisted by the FinEA finger in the Y direction; two properly-referenced identical laser sensors (Panasonic HL-G112-A-C5) to measure FinEA finger and cylindrical object displacements; a high voltage power supply (Ultravolt 20HVA24-BP1-F) to electrocally-activate the EA pad placed on the tested FinEA finger.

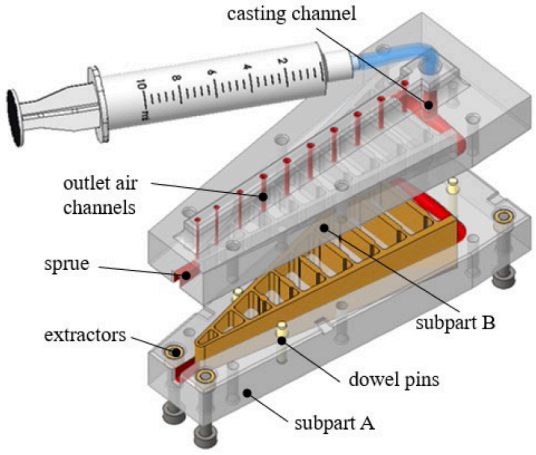

Fig. 6. Schematic of the molding setup.

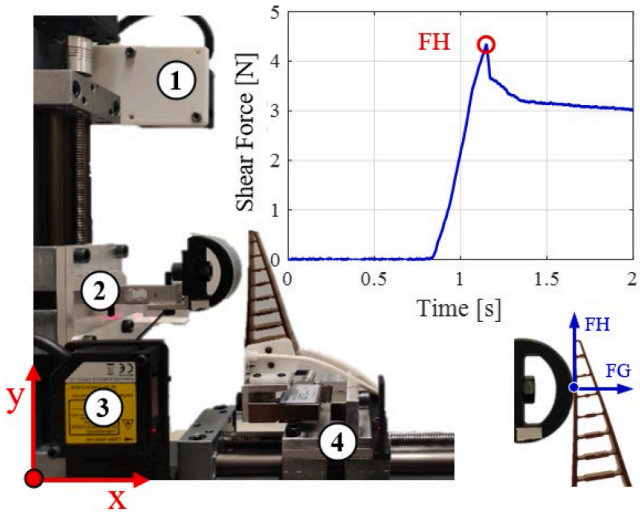

Fig. 7. Experimental setup: 1) laser to measure object motion in *Y* direction. 2) shear-type loadcell to measure FH. 3) laser to measure finger motion in *X* direction. 4) S-type loadcell to measure FG. The FH value corresponds to the peak of the shear-type loadcell reading during the vertical motion of the object occurring at constant speed.

Gripper performance was assessed based on the ratio between holding (FH) and grasping (FG) forces: a higher ratio meaning a better response as less clamping force (thus, less finger actuation effort and less object crushing) is required to hold a same object subjected to same external actions. As grasped objects, four half-cylinders with different diameters (50, 60, 70 and 80 mm) were 3D printed in Onyx® material and covered with a 100 μm thick PET film to provide a smooth uniform contact surface with the FinEA finger. A first round of test concerned the measurement of the mere friction contribution, obtained by keeping the EA pads unpowered (EA off). In the second round, a 4 kV DC voltage was applied across the EA pad electrodes, aiming at assessing the electro-adhesive performance (EA on). In each test, the finger was first displaced (in X direction) with a stroke of given magnitude, S, while keeping the object fixed, to achieve a given level of finger-cylinder contact. Upon completion of this movement, the FG value is obtained by reading the value acquired by the “S” type load cell. Then, the grasped object was moved upwards (in Y direction) at constant speed (2 mm/s), while keeping the finger fixed.

During this motion, the time evolution of the output of the shear beam load cell was acquired with 1000 Hz sampling rate (an exemplary measurement is shown in Fig. 7). From this data, the pull-off (breakaway) force, corresponding to the actual FH, was identified as the maximum force generated during the upwards object displacement. To build FH/FG variation curves, the procedure was repeated six times, with increasing finger strokes S: from 10 mm to 22.5 mm, with 2.5 mm increments.

6.2. Results and discussion

The FH vs. FG data collected during the testing of the new FinEA finger are reported in Fig. 8. For the sake of comparison, the original FinRay finger by FESTO was additionally tested with same procedure and conditions, and the related data are shown in Fig. 9(a). By analysing

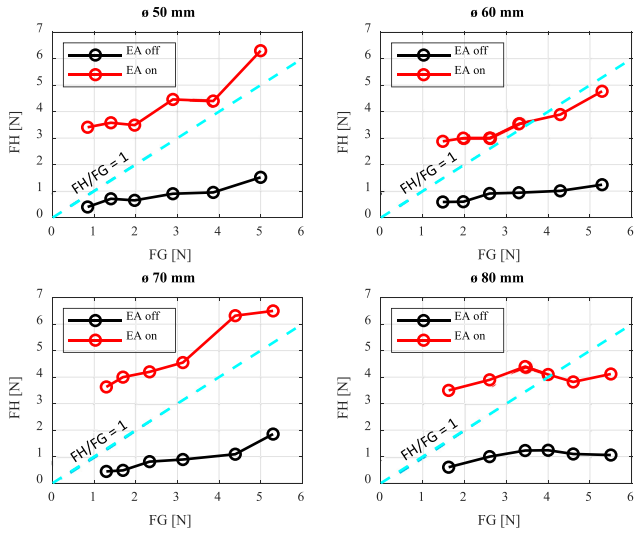

Fig. 8. FinEA holding vs. grasping force with EA on and off for each of the four considered cylindrical objects with diameters 50, 60, 70 and 80 mm.

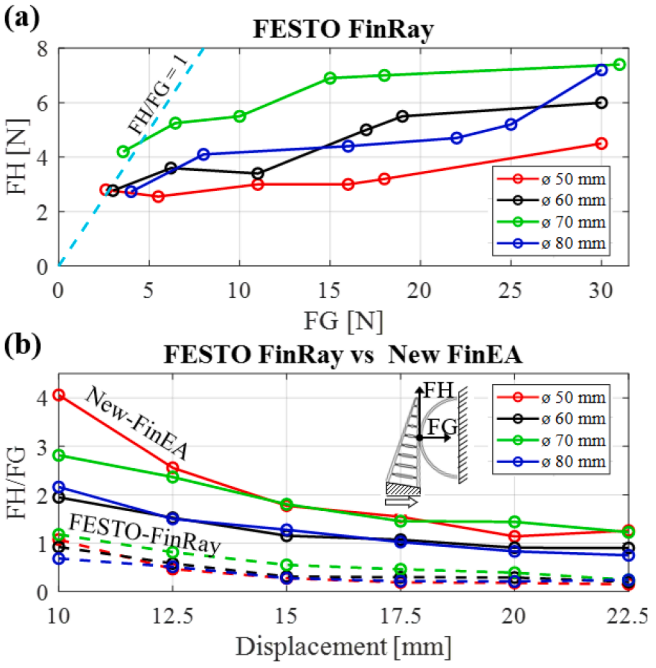

Fig. 9. (a) FESTO FinRay holding vs. grasping force for each of the four considered cylindrical objects with diameters 50, 60, 70 and 80 mm. (b) Comparison of the holding vs. grasping force ratio between FESTO FinRay and new FinEA, for each of the four considered cylindrical objects with diameters 50, 60, 70 and 80 mm over the tested finger stroke.

these results, the following can be observed:

- The maximum holding force (FH) exhibited by the two fingers is comparable, which ensures similar lifting capabilities.
- On an average basis, the grasping force (FG) of the new FinEA is five times lower than that of the FESTO FinRay, which enables the handling of softer and more fragile objects as well as reduces the force rating and the energy expenditure of the finger actuator.
- The new design combining a softer FinRay finger with EA pads provides a significant increase of the holding force, especially at full gripper stroke, which corresponds to finger maximum deformation and, thus, to the highest contact area.

To better compare the grasping performance of the two grippers, the line corresponding to the value FH/FG =1 was plotted on each of the graphs: while in the majority of the cases the new FinEA finger exhibits a ratio greater than one, the FESTO FinRay gripper mostly features a ratio lower than one. This comparison can be clearly observed in Fig. 9(b), where the ratio FH/FG of the two grippers is plotted for each value of the tested finger stroke.

Nonetheless, the similarity in FH values obtained with the two grippers demonstrates that the lower holding action caused by the use of a more compliant finger material is fully compensated by the electro-adhesion shear force contribution of the pad. In other words, the new proposed gripper, with same geometry and dimensions of the one provided by FESTO, features the same lifting capability, while applying a very low compressive force on the grasped object. The latter characteristic:

1) Makes the new FinEA gripper suitable for manipulating delicate, fragile and deformable objects, without wrinkling the surfaces. A clear exhibition of this behavior is shown in Fig. 10, where a set of different delicate products were grasped through the new FinEA gripper.
2) Provides the new FinEA gripper with similar lifting performance to that of the original FESTO FinRay, but with lower finger actuation forces, which can result in gripping energy savings in the order of 81, 65, 67, 72% respectively for each of the cylindrical objects 50, 60, 70, 80 mm.

To assess the validity of the model described in Section 3, the tests reported in Section 6 were numerically simulated. Results for the maximum gripper deformations experienced in each test are shown in Fig. 11, which highlights a precise overlapping of the finger deflections predicted by the model to the real ones obtained during the experiments.

This confirms the appropriateness of the hyperelastic strain-energy function identification and of the finite element model setup. The simulated data also show that the maximum deformation experienced by the new FinEA finger is around 18 %.

7. Conclusion

In the development of soft grippers (SGs), it is crucial to identify the best trade-off between finger compliance and lifting capacity. Commonly, SGs are either excessively soft and, thus, unable to sustain high lifting forces or excessively stiff and, thus, unsuitable to handle delicate objects. The FinEA gripper proposed in this paper aims at closing the gap between lifting capacity and compliance, which are difficult to be pursued at the same time. This was achieved thanks to the development approach consisting in the following:

- Start from an existing SG characterized by high lifting forces, but lacking in compliance for the manipulation of delicate objects (namely, FESTO Fin Ray);
- Critical choice and accurate characterization of a suitable material for gripper structure to increase its compliance;
- Preliminary assessment of gripper performance by means of FE analyses;
- Filling the gap in lifting capacity by integrating custom electro-adhesive (EA) pads on the finger surfaces, which makes it possible to generate controllable shear forces by electrical activation;
- Testing of the new gripper and comparison with the existing SG.

Due to the increased compliance, the new FinEA gripper is capable of manipulating delicate and fragile objects without damaging or wrinkling their surfaces. Tested with objects with different dimensions, the new gripper demonstrated an average increase of 71 % of the holding vs. grasping force ratio if compared to the original FESTO FinRay. While applying similar holding forces, the new gripper exerts significantly

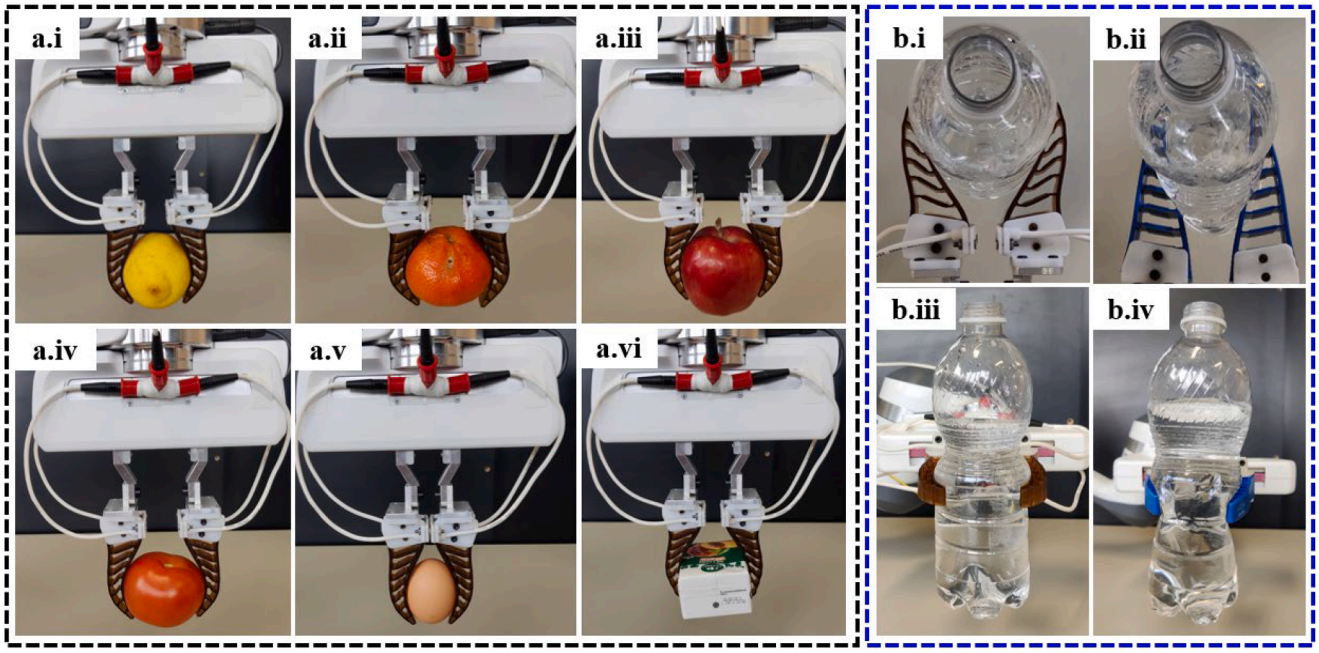

Fig. 10. Case studies on different products. (**a.i-a.vi**) Grasping of a lemon (156 g), a mandarin (154 g), an apple (207 g), a tomato (166 g), an egg (66 g) and a juice brik (226 g). Comparison of grasping a plastic bottle filled with water (384 g) by means of the new FinEA (**b.i, b.iii**) and the FESTO FinRay (**b.ii, b.iv**) grippers. Both the top and the front views highlight that the FESTO FinRay needs to deform and wrinkle the bottle (which is deliberately without the cap, to increase its compliance) to lift it. This does not occur with the new FinEA, which exploits the combination of soft finger material and electro-adhesion to lift the bottle without crushing it.

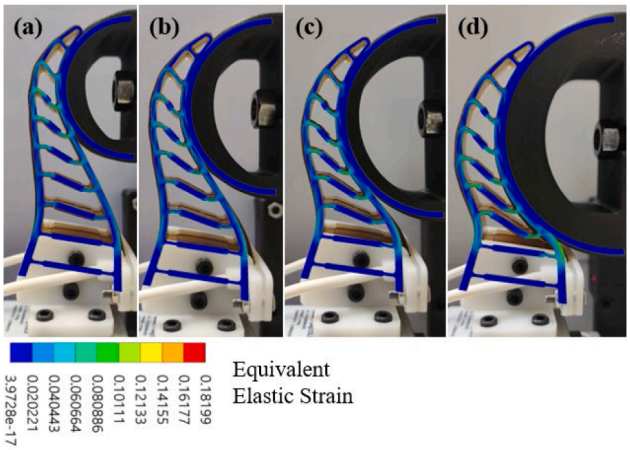

Fig. 11. Comparison between real and simulated deformations, for each of the cylindrical objects, 50, 60, 70, 80 mm. Respectively (a), (b), (c) and (d).

lower grasping force, with the twofold effect of reducing: i) compressive actions on the object; ii) the energy required for mechanical actuation.

CRediT authorship contribution statement

Amedeo Carloni: Conceptualization, Data curation, Formal analysis, Software, Writing – original draft. **Marcello Valori:** Conceptualization, Supervision, Writing – review & editing. **Federico Bertolucci:** Funding acquisition, Resources. **Lorenzo Agostini:** Conceptualization. **Giovanni Berselli:** Investigation, Supervision. **Irene Fassi:** Supervision. **Lorenzo Molinari Tosatti:** Supervision. **Rocco Vertechy:** Supervision.

Declaration of competing interest

The authors declare that they have no known competing financial interests or personal relationships that could have appeared to influence the work reported in this paper.

Data availability

Data will be made available on request.

Acknowledgment

This research was performed in collaboration with Adaptronics s.r.l. and funded by the following projects: UE FSE - REACT-EU - PON "Research and Innovation" 2014–2020 - D.M. MUR 1061/2021 - Action IV.5 – "PhD on Green reseach themes"; National Recovery and Resilience Plan (NRRP), Mission, 04 Component 2 Investment 1.5 - NextGenerationEU; INTELLIMAN (G.A.No. 101070136), Horizon Europe, Research and Innovation Programme. MICS (Made in Italy – Circular and Sustainable Extended Partnership and received funding from the European Union Next-GenerationEU (PIANO NAZIONALE DI RIPRESA E RESILIENZA (PNRR) – MISSIONE 4 COMPONENTE 2, INVESTIMENTO 1.3 – D.D. 1551.11-10-2022, PE00000004). This manuscript reflects only the authors' views and opinions, neither the European Union nor the European Commission can be considered responsible for them. The contribution of Simone Balestri in the simulation and experimental activities is also acknowledged.

References

[1] C. Melchiorri, M. Kaneko, Springer Handbook of Robotics, Springer, Berlin/Heidelberg, Germany, 2008, pp. 345–360.
[2] L. Birglen and T. Schlicht, "A statistical review of industrial robotic grippers," 2018, *Elsevier Ltd.* doi: 10.1016/j.rcim.2017.05.007.
[3] A. Hassan, M. Abomoharam, Modeling and design optimization of a robot gripper mechanism, Robot. Comput. Integr. Manuf. 46 (2017) 94–103, https://doi.org/10.1016/j.rcim.2016.12.012.
[4] T. Li, Y. Yan, C. Yu, J. An, Y. Wang, and G. Chen, "A comprehensive review of robot intelligent grasping based on tactile perception," 2024, *Elsevier Ltd.* doi: 10.1016/j.rcim.2024.102792.
[5] I. Hussain, et al., Modeling and prototyping of an underactuated gripper exploiting joint compliance and modularity, IEEE Robot. Autom. Lett. 3 (4) (2018) 2854–2861, https://doi.org/10.1109/LRA.2018.2845906.

[6] C. Liu, et al., Design of a self-adaptive gripper with rigid fingers for industrial internet, Robot. Comput. Integr. Manuf. 65 (2020), https://doi.org/10.1016/j.rcim.2020.101976.
[7] H. Dong, E. Asadi, C. Qiu, J. Dai, I.M. Chen, Geometric design optimization of an under-actuated tendon-driven robotic gripper, Robot. Comput. Integr. Manuf. 50 (2018) 80–89, https://doi.org/10.1016/j.rcim.2017.09.012.
[8] J. Shintake, V. Cacucciolo, D. Floreano, and H. Shea, "Soft robotic grippers," 2018, *Wiley-VCH Verlag*. doi: 10.1002/adma.201707035.
[9] S. Zaidi, M. Maselli, C. Laschi, and M. Cianchetti, "Actuation technologies for soft robot grippers and manipulators: a review", doi: 10.1007/s43154-021-00054-5/Published.
[10] S. Terrile, M. Argüelles, and A. Barrientos, "Comparison of different technologies for soft robotics grippers," 2021, *MDPI AG*. doi: 10.3390/s21093253.
[11] B. Zhang, Y. Xie, J. Zhou, K. Wang, and Z. Zhang, "State-of-the-art robotic grippers, grasping and control strategies, as well as their applications in agricultural robots: a review," 2020, *Elsevier B.V.* doi: 10.1016/j.compag.2020.105694.
[12] Y. Hao, Y. Visell, Beyond soft hands: efficient grasping with non-anthropomorphic soft grippers, Front. Robot. AI. 8 (2021), https://doi.org/10.3389/frobt.2021.632006.
[13] T. Sun, Y. Chen, T. Han, C. Jiao, B. Lian, Y. Song, A soft gripper with variable stiffness inspired by pangolin scales, toothed pneumatic actuator and autonomous controller, Robot. Comput. Integr. Manuf. 61 (2020), https://doi.org/10.1016/j.rcim.2019.101848.
[14] S. D'Avella, P. Tripicchio, C.A. Avizzano, A study on picking objects in cluttered environments: exploiting depth features for a custom low-cost universal jamming gripper, Robot. Comput. Integr. Manuf. 63 (2020), https://doi.org/10.1016/j.rcim.2019.101888.
[15] Y. Fan, B. Yi, and D. Liu, "An overview of stiffening approaches for continuum robots," 2024, *Elsevier Ltd*. doi: 10.1016/j.rcim.2024.102811.
[16] B. Mosadegh, et al., Pneumatic networks for soft robotics that actuate rapidly, Adv. Funct. Mater. 24 (15) (2014) 2163–2170, https://doi.org/10.1002/adfm.201303288.
[17] M. Manti, T. Hassan, G. Passetti, N. D'Elia, C. Laschi, M. Cianchetti, A bioinspired soft robotic gripper for adaptable and effective grasping, Soft. Robot. 2 (3) (2015) 107–116, https://doi.org/10.1089/soro.2015.0009.
[18] J. Shintake, B. Schubert, S. Rosset, H. Shea, D. Floreano, Variable stiffness actuator for soft robotics using dielectric elastomer and low-melting-point alloy, in: IEEE International Conference on Intelligent Robots and Systems, Institute of Electrical and Electronics Engineers Inc., 2015, pp. 1097–1102, https://doi.org/10.1109/IROS.2015.7353507.
[19] O.A. Araromi, et al., Rollable multisegment dielectric elastomer minimum energy structures for a deployable microsatellite gripper, IEEE/ASME Trans. Mechatron. 20 (1) (2015) 438–446, https://doi.org/10.1109/TMECH.2014.2329367.
[20] G.J. Monkman, "An Analysis of Astrictive Prehension".
[21] B.N.J. Persson, General theory of electroadhesion, J. Phys. Condens. Matter 33 (43) (2021), https://doi.org/10.1088/1361-648X/abe797.
[22] I.D. Sîrbu, et al., Adhesion state estimation for electrostatic gripper based on online capacitance measure, Actuators. 11 (10) (2022), https://doi.org/10.3390/act11100283.
[23] V. Cacucciolo, H. Shea, G. Carbone, Peeling in electroadhesion soft grippers, Extreme Mech. Lett. 50 (2022), https://doi.org/10.1016/j.eml.2021.101529.
[24] N. Berdozzi, et al., Rapid fabrication of electro-adhesive devices with inkjet printed electrodes, IEEE Robot. Autom. Lett. 5 (2) (2020) 2770–2776, https://doi.org/10.1109/LRA.2020.2972838.
[25] L. Zhou, L. Ren, Y. Chen, S. Niu, Z. Han, and L. Ren, "Bio-inspired soft grippers based on impactive gripping," 2021, *John Wiley and Sons Inc*. doi: 10.1002/advs.202002017.
[26] J. Shintake, S. Rosset, B. Schubert, D. Floreano, H. Shea, Versatile soft grippers with intrinsic electroadhesion based on multifunctional polymer actuators, Adv. Mater. 28 (2) (2016) 231–238, https://doi.org/10.1002/adma.201504264.
[27] J. Guo, K. Elgeneidy, C. Xiang, N. Lohse, L. Justham, J. Rossiter, Soft pneumatic grippers embedded with stretchable electroadhesion, Smart. Mater. Struct. 27 (5) (2018), https://doi.org/10.1088/1361-665X/aab579.
[28] V. Alizadehyazdi, M. Bonthron, M. Spenko, An electrostatic/gecko-inspired adhesives soft robotic gripper, IEEE Robot. Autom. Lett. 5 (3) (2020) 4679–4686, https://doi.org/10.1109/LRA.2020.3003773.
[29] R. Bannasch and L. Kniese, "Manipulator tool and holding and/or expanding tool with at least one manipulator tool.," Patent US8333417, 2012.
[30] X. Shan, L. Birglen, Modeling and analysis of soft robotic fingers using the fin ray effect, Int. J. Robot. Res. 39 (14) (2020) 1686–1705, https://doi.org/10.1177/0278364920913926.
[31] R. Chen, et al., Bio-inspired shape-adaptive soft robotic grippers augmented with electroadhesion functionality, Soft. Robot. 6 (6) (2019) 701–712, https://doi.org/10.1089/soro.2018.0120.
[32] W. Ruotolo, D. Brouwer, and M.R. Cutkosky, "From grasping to manipulation with gecko-inspired adhesives on a multifinger gripper," 2021. [Online]. Available: https://www.science.org.
[33] L. Marechal, P. Balland, L. Lindenroth, F. Petrou, C. Kontovounisios, F. Bello, Toward a common framework and database of materials for soft robotics, Soft. Robot. 8 (3) (2021) 284–297, https://doi.org/10.1089/soro.2019.0115.
[34] R.W. Ogden, G. Saccomandi, I. Sgura, Fitting hyperelastic models to experimental data, Comput. Mech. 34 (6) (2004) 484–502, https://doi.org/10.1007/s00466-004-0593-y.
[35] M.S. Xavier, A.J. Fleming, Y.K. Yong, Finite element modeling of soft fluidic actuators: overview and recent developments, Adv. Intell. Syst. 3 (2) (2021) 2000187, https://doi.org/10.1002/aisy.202000187.
[36] J. Bergström, 5 - Elasticity/hyperelasticity, in: J. Bergström (Ed.), Mechanics of Solid Polymers, William Andrew Publishing, 2015, pp. 209–307, https://doi.org/10.1016/B978-0-323-31150-2.00005-4.